Hindawi Publishing Corporation
Mathematical Problems in Engineering
Volume 2015, Article ID 960678, 12 pages
http://dx.doi.org/10.1155/2015/960678

Research Article

A Novel Torque Coordination Control Strategy of a Single-Shaft Parallel Hybrid Electric Vehicle Based on Model Predictive Control

Jing Sun,[1,2] Guojing Xing,[1] Xudong Liu,[1] Xiaoling Fu,[1,3] and Chenghui Zhang[1]

[1] *School of Control Science and Engineering, Shandong University, Jinan 250061, China*
[2] *School of Information and Electronic Engineering, Shandong Institute of Business and Technology, Yantai 264005, China*
[3] *Department of Physics, Changji University, Changji 831100, China*

Correspondence should be addressed to Chenghui Zhang; zchui@sdu.edu.cn

Received 23 January 2014; Accepted 24 June 2014

Academic Editor: Leonid Shaikhet

The torque coordination control during mode transition is a very important task for hybrid electric vehicle (HEV) with a clutch serving as the key enabling actuator element. Poor coordination will deteriorate the drivability of the driver and lead to excessive wearing to the clutch friction plates. In this paper, a novel torque coordination control strategy for a single-shaft parallel hybrid electric vehicle is presented to coordinate the motor torque, engine torque, and clutch torque so that the seamless mode switching can be achieved. Different to the existing model predictive control (MPC) methods, only one model predictive controller is needed and the clutch torque is taken as an optimized variable rather than a known parameter. Furthermore, the successful idea of model reference control (MRC) is also used for reference to generate the set-point signal required by MPC. The parameter sensitivity is studied for better performance of the proposed model predictive controller. The simulation results validate that the proposed novel torque coordination control strategy has less vehicle jerk, less torque interruption, and smaller clutch frictional losses, compared with the baseline method. In addition, the sensitivity and adaptiveness of the proposed novel torque coordination control strategy are evaluated.

1. Introduction

HEV represents an effective solution to significantly reduce the consumption of fossil fuels and carbon emissions [1], whose control problem is generally regarded as an energy management optimization problem to minimize the fuel consumption and the exhaust emissions over an arbitrary driving cycle. Many researches have focused on the energy management strategy (EMS) which aims to improve fuel economies and reduce emissions [1–8]. However, to our knowledge, the drivability and smoothness are often disregarded in energy management strategies. In fact, HEV should be regarded not only for its fuel saving potential but also for its additional driving comfort and add on performance. To improve the HEV's fuel economies, the optimized vehicle operations require frequent mode switching which will cause impact and jitter to the powertrain. For the clutch-enabled HEV, one special challenge in managing mode transition is the switch from pure electric running to parallel hybrid operation, as the clutch friction torque introduces nonlinear dynamics to the powertrain. Sharp torque variation may occur at this time due to the abrupt introduction of the engine torque into the driveline by a controlled clutch torque. Obviously, the driving comfort of the driver will be deteriorated and the clutch lifespan will be shortened unless the transition process is carefully controlled. The core problem of the mode transition process is torque coordination control which is a critical control task for HEV drivability and clutch lifespan.

As far as we know, Tong defined the control issue of how to coordinate engine and motor under mode transition as a coordinated control issue for the first time and proposed engine torque open-loop control with dynamical engine torque estimation and motor torque compensation [9]. Davis and Lorenz built engine state observer and cancelled the

engine torque ripple using integrated starter alternator [10]. Wang et al. limited the changing rate of the load signal of engine and motor to decrease the torque fluctuation of mode transition process [11]. Li et al. proposed a model matching control method for the dynamic coordinated control of a parallel hybrid electric vehicle [12]. In the aforementioned works, the difference of dynamic response characteristic between engine and electric motor was considered, and the fast response characteristic of motor was used to compensate the engine. Nevertheless, the clutch dynamic characteristic which is a crucial factor to the mode transition performance is neglected in the above works.

Taking the clutch dynamic characteristic into account, many research works handled the torque coordination problem from the perspective of state equations under different running modes. To achieve a seamless transition from pure electric running to parallel hybrid operation of HEV, Wang et al. applied a fuzzy adaptive sliding mode approach to the mode transition control for a series-parallel hybrid electric bus [13]. Koprubasi et al. applied switched hybrid theory to the control of a simplified model of a parallel hybrid electric vehicle drivetrain [14]. Minh and Rashid built up a typical model of a parallel hybrid electric vehicle and developed two model predictive controllers for this model to control the speeds and torques for fast clutch engagement [15]. This paper finished the preparation phase for the clutch slipping friction phase but did not involve the control during the clutch slipping friction phase. Beck et al. also applied two model predictive controllers to regulate HEV mode transitions [16]. Nevertheless, in the aforementioned works, the clutch normal pressure in its slipping friction phase, which is proportional to clutch torque and plays a crucial role for the improvement of transition performance, was viewed as a known parameter and its optimizing function was neglected. In fact, the clutch torque in the slipping friction phase can be controlled independently by its actuator [17] and thus can be used as an optimized control variable. To coordinate the motor torque, engine torque, and clutch torque to manage transitions, Chen et al. proposed a MRC law [18] which is a very valuable idea.

Obviously, as an important and gordian knot, torque coordination control has already caused the extensive concerns of the academia and business circles.

MPC, which can be regarded as a kind of optimal control methods, is one of the most practical advanced control techniques in industrial applications [19]. At each sampling time, it employs a dynamic model of plant to forecast the future behavior of states and determines the future control action according to optimization of a certain performance target function or an operating cost function. MPC possesses the advantages including robustness, simplicity of modeling, and good capability of handling constraints, so it can ensure a satisfying system performance [20]. MPC has been successfully applied in many engineering problems, such as the electrical motor drive system [21], the power plant coordinate control [22], and the vehicle active steering system [23]. Several automotive companies have contributed and supported MPC research, including Ford, BMW, Honda, Honeywell, PSA, and Toyota [24].

This paper proposes a novel torque coordination control strategy for the typical switching from pure electric running to parallel hybrid operation for a single-shaft parallel HEV based on MPC. The design objective is to coordinate the engine torque, the motor torque, and the clutch torque to achieve smooth transition with reduced driveline jerk and clutch frictional losses. The innovations of this paper are outlined as follows. Firstly, only one model predictive controller is needed compared with the existing MPC methods about torque coordination control in [15, 16], which is helpful to reduce the computation burden. Secondly, as a pivotal factor, the clutch torque is used as an optimized variable rather than a known parameter in MPC, which will increase the design degree of freedom. Lastly, the successful experience of MRC in [18] is introduced into the proposed novel torque coordination control strategy, and the transient output of the reference model is used as the set-point signal of MPC algorithm. The simulation results show that the proposed novel torque coordination control strategy can achieve smoother transition with less driveline torque interruption and smaller clutch frictional losses compared with the outcomes of the conventional method.

The remainder of this paper is organized as follows. Section 2 establishes the HEV dynamic models during different running modes. Section 3 introduces the block diagram and detailed implementation of the proposed novel torque coordination control strategy for the mode transition from pure electric running to parallel hybrid operation. In Section 4, the results of the proposed torque coordination control strategy are compared with those of the conventional method, and the sensitivity and adaptiveness of the proposed novel strategy are also evaluated. The paper is concluded in Section 5.

2. HEV Modeling

It is well known that the well-built dynamic model is the precondition of the analysis and control to HEV powertrain. To implement the proposed novel torque coordination control strategy, a control-oriented HEV model capturing the mode transition dynamics will be built in this section.

Figure 1 shows the configuration of the single-shaft parallel hybrid powertrain to be studied in this paper. It consists of a conventional engine, an integrated starter and generator (ISG), and a traction motor. A clutch separates the powertrain into two parts. The first part includes the engine and the ISG, and the second part consists of the traction motor and the rest of the transmission. The driven wheels are connected with a standard automated transferred gearbox and a differential gearbox.

When HEV runs at low speeds (below 30 km/h), the powertrain runs in pure electric mode. At this time, the clutch is open and the traction motor drives the vehicle using solely electric energy from the battery. The transition from pure electric running to parallel hybrid operation takes place at high speeds (above 30 km/h) by closing the clutch when the traction motor is no longer sufficient to propel the vehicle. In the hybrid driving mode, the clutch is locked and the traction motor drives the vehicle together with the engine.

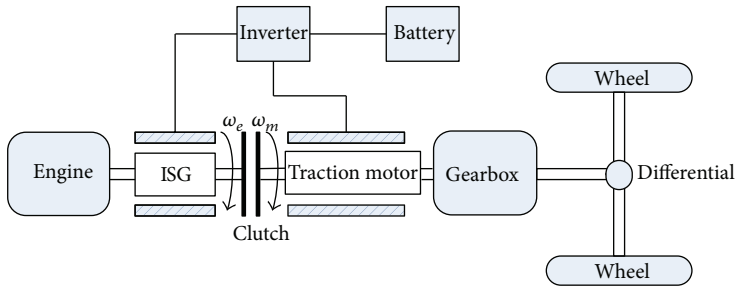

Figure 1: Configuration of a single-shaft parallel hybrid powertrain.

2.1. Vehicle Resistance Model. The vehicle resistance model is composed of three separate parts: the rolling resistance, the air drag, and the combined mechanical losses in gearbox, differential, and shaft bearings due to friction. The third part can be approximated from measured characteristic curves as a second order polynomial. The resulting resistance torque T_{wh} can be expressed as follows:

$$T_{wh} = \left[mg\sin\alpha + f_r mg\cos\alpha + \frac{\rho}{2} c_D A_V (\omega_{wh} R)^2 \right] R + a_0 + a_1\omega_{wh} + a_2\omega_{wh}^2, \quad (1)$$

where m is the vehicle mass, g is the gravitational acceleration constant, α is the road inclination angle, f_r is the tire rolling resistance coefficient, ρ is the air density, c_D is the aerodynamic drag coefficient, A_V is the vehicle frontal area, ω_{wh} is the vehicle speed, R is the tire dynamic rolling radius, and a_0, a_1, a_2 are the transmission friction curve fitting factors. The linearization $T_{wh} = T_{wh0} + a_1\omega_{wh}$ is reasonable without significant loss of accuracy since the developed powertrain model is used for low vehicle speeds and the terms proportional to ω_{wh}^2 have less contributions to T_{wh} [16]. The vehicle mass m, the road inclination angle α, and the tire rolling resistance coefficient f_r can be considered to be constant during the short mode transiton process, so $T_{wh0} = (mg\sin\alpha + f_r mg\cos\alpha)R + a_0$ can be seen as the constant part of vehicle resistance. Since the actual mode transition may occur under different road inclination angel, vehicle mass, or tire rolling resistance coefficient, the adaptiveness of the proposed torque coordination control strategy to these factors will be discussed in Section 4.

2.2. Clutch Model. The clutch engagement process can be divided into three phases, namely, the open phase, the slipping friction phase, and the locked phase.

When the clutch is open, the two sides of clutch are not contacted. Thus the open phase is not important to the vehicle dynamics and the clutch torque $T_c = 0$ at this circumstance.

When the clutch is engaged and the clutch primary speed is not equal to the clutch secondary speed, the clutch is in the slipping friction phase, during which the vehicle longitudinal dynamics are sensitive to the clutch torque profile. In this case, the clutch torque T_c can be expressed as follows [25]:

$$T_c = \mu_s \cdot F_c \cdot R_c \cdot \operatorname{sign}(\omega_p - \omega_s), \quad (2)$$

where μ_s is the slipping friction coefficient of clutch, F_c is the clutch normal pressure, R_c is the equivalent acting radius of the friction torque on clutch plate, ω_p is the clutch primary speed, ω_s is the clutch secondary speed, and sign(·) is a signum function.

When the clutch primary speed is equal to the clutch secondary speed, the clutch is locked, and the clutch torque no longer affects the vehicle dynamics. Moreover, T_c can be derived from the dynamics of the powertrain and is subject to $T_c \in [-\mu_l \cdot F_c \cdot R_c, \mu_l \cdot F_c \cdot R_c]$, where μ_l is the static friction coefficient of the clutch.

2.3. HEV Dynamic Models during Different Running Modes. The transition from pure electric running to parallel hybrid operation is classified as the following four modes.

Mode 1. When the vehicle speed is lower than 30 km/h, the clutch is open. The vehicle is solely propelled by the traction motor and the engine is unstarted.

Neglecting the torsional displacement of the half shafts and assuming that the differential gear ratio is 1, the state-space equation during this phase can be denoted by

$$J_m'\dot{\omega}_m = T_m - b_m\omega_m - \frac{1}{i}\left(T_{wh0} + \frac{a_1\omega_m}{i}\right), \quad \omega_e = 0, \quad (3)$$

where $J_m' = J_m + J_c + J_{gb} + (mR^2/i^2)$ is the combined inertia of the motor, the clutch, the gearbox, and the transmission at the motor shaft (J_m is the inertia of the motor, J_c is the inertia of the clutch, and J_{gb} is the inertia of the gearbox), ω_m is the traction motor speed, T_m is the traction motor torque, b_m is the traction motor friction coefficient, i is the gear ratio, and ω_e is the engine speed.

Mode 2. When the vehicle speed exceeds 30 km/h, the clutch remains open. The vehicle is still propelled by the traction motor separately and the engine is started with the help of ISG to its idle speed which is generally 800 r/min.

The state-space equation during this phase can be denoted by

$$J_m'\dot{\omega}_m = T_m - b_m\omega_m - \frac{1}{i}\left(T_{wh0} + \frac{a_1\omega_m}{i}\right), \quad J_e'\dot{\omega}_e = T_e - b_e\omega_e, \quad (4)$$

where J_e' is the total inertia moment of engine and ISG, b_e is the engine friction coefficient, and T_e denotes the total torque of engine and ISG (the internal dynamics of engine and ISG are ignored here for simplicity).

Mode 3. When the speed difference between two sides of the clutch is less than a given threshold value, the clutch enters into the slipping friction phase. As a transitional stage from pure electric running to parallel hybrid operation, this is the most important phase to coordinate the motor torque, the clutch torque, and the engine torque for improved drivability and reduced clutch frictional losses.

The state-space equation during this phase can be denoted by

$$\begin{aligned} J_m'\dot{\omega}_m &= T_m + T_c - b_m\omega_m - \frac{1}{i}\left(T_{wh0} + \frac{a_1\omega_m}{i}\right), \\ J_e'\dot{\omega}_e &= T_e - b_e\omega_e - T_c. \end{aligned} \tag{5}$$

As is shown in (5), the clutch frictional torque T_c begins to affect the dynamic characteristics of the powertrain. It is notable that T_c in the slipping friction phase was viewed as a known parameter in the existing MPC methods about torque coordination control. In fact, it can be controlled independently by its actuator in the slipping friction phase. T_c will be used as an optimized control variable in the proposed novel torque coordination control strategy based on MPC, which will increase the control flexibility.

Mode 4. When the speed difference between two sides of the clutch equals zero (i.e. $\omega_m = \omega_e$), the cultch is locked, and the clutch enters into the static friction phase.

The state-space equation in this phase can be denoted by

$$\left(J_e' + J_m'\right)\dot{\omega}_m = T_e + T_m - \left(b_e + b_m\right)\omega_m - \frac{1}{i}\left(T_{wh0} + \frac{a_1\omega_m}{i}\right). \tag{6}$$

3. The Model Predictive Controller Design

A block diagram of the proposed novel torque coordination control strategy is shown in Figure 2. Different to the existing MPC methods about torque coordination control in [15, 16], only one model predictive controller is needed and the clutch torque T_c is used as an optimized variable rather than a known parameter to improve the performance of MPC. The idea of MRC in [18] is used for reference in the proposed novel strategy. The reference model is built to capture the desired powertrain dynamics of the pure electric mode. The input of reference model is the equivalent driver's demand torque determined by the acceleration pedal. The transient output of the reference model is used as the target output of the plant (i.e., the set-point signal of MPC algorithm). The control goal is that both the clutch primary speed (i.e., ω_e) and the clutch secondary speed (i.e., ω_m) can track the output of the reference model. This will not only assure that the clutch primary speed is always equal to the clutch secondary speed to reduce clutch wear during the slipping friction phase, but also assure that the vehicle runs as if it were still in pure electric mode to reduce the longitudinal jerk and assure driving comfort.

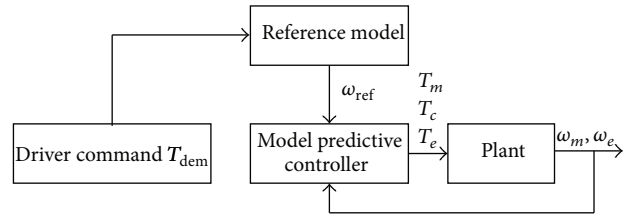

Figure 2: The structure of the proposed novel torque coordination control strategy.

Let ε represent the speed difference of the two sides of the clutch; that is, $\varepsilon = \omega_m - \omega_e$; the proposed control strategy can be described as follows.

When ε is larger than a predefined threshold, the vehicle runs in mode 2. The traction motor propels the vehicle alone.

When ε is smaller than this threshold, the vehicle runs in mode 3. The engine torque, the clutch torque, and the traction motor torque are all determined by the model predictive controller.

When ε is equal to zero, the vehicle runs in mode 4. The engine torque and the traction motor torque are determined by EMS and the clutch torque is no longer controllable.

The discrete-time model predictive control algorithm is used here, since it is convenient to be implemented in the current digitalized vehicle control units. Let T_s denote the sampling time interval; then the discrete form of state-space equation (5) in mode 3 is

$$\begin{aligned} \omega_m(k+1) &= \left(1 - \frac{b_m T_s}{J_m'} - \frac{a_1 T_s}{J_m' i^2}\right)\omega_m(k) \\ &\quad + \frac{T_s}{J_m'}T_m(k) + \frac{T_s}{J_m'}T_c(k) - \frac{T_{wh0}T_s}{J_m' i}, \\ \omega_e(k+1) &= \left(1 - \frac{b_e T_s}{J_e'}\right)\omega_e(k) - \frac{T_s}{J_e'}T_c(k) + \frac{T_s}{J_e'}T_e(k). \end{aligned} \tag{7}$$

System (7) can be rewritten in the following matrix form:

$$\begin{aligned} \begin{bmatrix} \omega_m(k+1) \\ \omega_e(k+1) \end{bmatrix} &= \begin{bmatrix} 1 - \frac{b_m T_s}{J_m'} - \frac{a_1 T_s}{J_m' i^2} & 0 \\ 0 & 1 - \frac{b_e T_s}{J_e'} \end{bmatrix} \begin{bmatrix} \omega_m(k) \\ \omega_e(k) \end{bmatrix} \\ &\quad + \begin{bmatrix} \frac{T_s}{J_m'} & \frac{T_s}{J_m'} & 0 \\ 0 & -\frac{T_s}{J_e'} & \frac{T_s}{J_e'} \end{bmatrix} \begin{bmatrix} T_m(k) \\ T_c(k) \\ T_e(k) \end{bmatrix} \\ &\quad + \begin{bmatrix} -\frac{T_{wh0}T_s}{J_m' i} \\ 0 \end{bmatrix}. \end{aligned} \tag{8}$$

It can be seen that this plant has 2 states and 3 inputs. The introduced input variable $T_c(k)$ is to be optimized that

is significantly different to the existing MPC methods about torque coordination control.

Let

$$x_d(k) = \begin{bmatrix} \omega_m(k) \\ \omega_e(k) \end{bmatrix}; \tag{9}$$

then (8) can be rewritten as the following form:

$$x_d(k+1) = A_d x_d(k) + B_d u(k) + B_\xi \xi, \tag{10}$$

where

$$A_d = \begin{bmatrix} 1 - \frac{b_m T_s}{J'_m} - \frac{a_1 T_s}{J'_m i^2} & 0 \\ 0 & 1 - \frac{b_e T_s}{J'_e} \end{bmatrix},$$

$$B_d = \begin{bmatrix} \frac{T_s}{J'_m} & \frac{T_s}{J'_m} & 0 \\ 0 & -\frac{T_s}{J'_e} & \frac{T_s}{J'_e} \end{bmatrix}, \tag{11}$$

$$B_\xi \xi = \begin{bmatrix} -\frac{T_{wh0} T_s}{J'_m i} \\ 0 \end{bmatrix}.$$

Applying the differential operator to both sides of (10) yields [26, 27]

$$\begin{aligned} x_d(k+1) - x_d(k) = {} & A_d\left(x_d(k) - x_d(k-1)\right) \\ & + B_d\left(u(k) - u(k-1)\right). \end{aligned} \tag{12}$$

The state increment is defined as

$$\Delta x_d(k) = x_d(k) - x_d(k-1), \tag{13}$$

and the control increment is defined as

$$\Delta u(k) = u(k) - u(k-1). \tag{14}$$

Thus (12) can be denoted by

$$\Delta x_d(k+1) = A_d \Delta x_d(k) + B_d \Delta u(k). \tag{15}$$

Let the following new state vector be

$$x(k) = \left[\Delta x_d(k)^T \quad x_d(k)^T\right]^T, \tag{16}$$

where the superscript T indicates matrix transpose. The following augmented model can be obtained:

$$\begin{aligned} \begin{bmatrix} \Delta x_d(k+1) \\ x_d(k+1) \end{bmatrix} &= \begin{bmatrix} A_d & 0_d^T \\ A_d & I \end{bmatrix} \begin{bmatrix} \Delta x_d(k) \\ x_d(k) \end{bmatrix} + \begin{bmatrix} B_d \\ B_d \end{bmatrix} \Delta u(k), \\ y(k) &= \begin{bmatrix} 0_d & I \end{bmatrix} \begin{bmatrix} \Delta x_d(k) \\ x_d(k) \end{bmatrix}. \end{aligned} \tag{17}$$

The output dimension of (17) is 2. The state dimension of (17) is 4. I is the identity matrix with dimensions 2×2 and 0_d is a 2×2 zero matrix.

Let

$$A = \begin{bmatrix} A_d & 0_d^T \\ A_d & I \end{bmatrix}, \quad B = \begin{bmatrix} B_d \\ B_d \end{bmatrix}, \quad C = \begin{bmatrix} 0_d & I \end{bmatrix}; \tag{18}$$

then (17) can be rewritten in the following form:

$$\begin{aligned} x(k+1) &= Ax(k) + B\Delta u(k), \\ y(k) &= Cx(k), \end{aligned} \tag{19}$$

where

$$x(k) = \begin{bmatrix} \Delta\omega_m(k) \\ \Delta\omega_e(k) \\ \omega_m(k) \\ \omega_e(k) \end{bmatrix},$$

$$A = \begin{bmatrix} 1 - \frac{b_m T_s}{J'_m} - \frac{a_1 T_s}{J'_m i^2} & 0 & 0 & 0 \\ 0 & 1 - \frac{b_e T_s}{J'_e} & 0 & 0 \\ 1 - \frac{b_m T_s}{J'_m} - \frac{a_1 T_s}{J'_m i^2} & 0 & 1 & 0 \\ 0 & 1 - \frac{b_e T_s}{J'_e} & 0 & 1 \end{bmatrix}, \tag{20}$$

$$B = \begin{bmatrix} \frac{T_s}{J'_m} & \frac{T_s}{J'_m} & 0 \\ 0 & -\frac{T_s}{J'_e} & \frac{T_s}{J'_e} \\ \frac{T_s}{J'_m} & \frac{T_s}{J'_m} & 0 \\ 0 & -\frac{T_s}{J'_e} & \frac{T_s}{J'_e} \end{bmatrix}, \quad C = \begin{bmatrix} 0 & 0 & 1 & 0 \\ 0 & 0 & 0 & 1 \end{bmatrix}.$$

N_p and N_c are used to represent the prediction horizon and the control horizon, respectively. When N_c is less than N_p, at the sample time k, $u(k+i)$ $(i = 0, 1, \ldots, N_p - 1)$ keeps invariant after $i = N_c - 1$ [28]. The well-known disadvantage of MPC method is that the calculation of control action requires a cumbersome computation load since it requires the solution of an optimization problem at each sampling time. N_p and N_c determine the computation load to a great extent. To reduce the computation burden, N_p is chosen to be 3, and N_c is chosen to be 1; thus $u(k+2) = u(k+1) = u(k)$. The future state variables can be sequentially calculated based on the state-space model (A, B, C):

$$\begin{aligned} x(k+1 \mid k) &= Ax(k) + B\Delta u(k), \\ x(k+2 \mid k) &= A^2 x(k) + AB\Delta u(k) + B\Delta u(k+1) \\ &= A^2 x(k) + AB\Delta u(k), \\ x(k+3 \mid k) &= A^3 x(k) + A^2 B\Delta u(k) \\ &\quad + AB\Delta u(k+1) + B\Delta u(k+2) \\ &= A^3 x(k) + A^2 B\Delta u(k). \end{aligned} \tag{21}$$

On the basis of the predicted state variables, the predicted output variables can be indicated by

$$\begin{aligned} y(k+1 \mid k) &= CAx(k) + CB\Delta u(k), \\ y(k+2 \mid k) &= CA^2x(k) + CAB\Delta u(k), \\ y(k+3 \mid k) &= CA^3x(k) + CA^2B\Delta u(k). \end{aligned} \tag{22}$$

Defining vectors

$$\begin{aligned} Y &= \left[y(k+1 \mid k)^T \quad y(k+2 \mid k)^T \quad y(k+3 \mid k)^T\right]^T \\ &= \left[\omega_m(k+1 \mid k), \omega_e(k+1 \mid k), \omega_m(k+2 \mid k),\right. \\ &\qquad \left.\omega_e(k+2 \mid k), \omega_m(k+3 \mid k), \omega_e(k+3 \mid k)\right]^T, \\ \Delta U &= \Delta u(k) = \left[\Delta T_m(k) \quad \Delta T_c(k) \quad \Delta T_e(k)\right]^T, \end{aligned} \tag{23}$$

then (22) can be expressed as the following compact matrix form:

$$Y = Fx(k) + \phi\Delta U, \tag{24}$$

where

$$F = \begin{bmatrix} CA \\ CA^2 \\ CA^3 \end{bmatrix}, \qquad \phi = \begin{bmatrix} CB \\ CAB \\ CA^2B \end{bmatrix}. \tag{25}$$

At the sample time k, the objective of MPC is to bring the predicted outputs $\omega_m(k+i \mid k)$ $(i = 1,2,3)$ and $\omega_e(k+i \mid k)$ $(i = 1,2,3)$ as close as possible to the set-point signal $r(k)$. To generate an ideal $r(k)$ required by MPC, the idea of MRC in [18] is introduced. To achieve a smooth mode transition from pure electric running to parallel hybrid operation, the vehicle is expected to run as if it were still in the pure electric running. This desired performance can be expressed by a reference model that will be mimicked by the plant through MPC. Because the clutch is indeed locked when the engagement is completed, the clutch is assumed to be locked in the reference model; thus, the desired clutch primary speed is equal to the clutch secondary speed. The dynamic equation of the reference model is

$$\left(J_e' + J_m'\right)\dot{\omega}_{\text{ref}} = T_{\text{dem}} - \left(b_e + b_m\right)\omega_{\text{ref}} - \frac{1}{i}\left(T_{wh0} + \frac{a_1\omega_{\text{ref}}}{i}\right), \tag{26}$$

where T_{dem} is the equivalent driver's demand torque with respect to gearbox input side and ω_{ref} is the output of the reference model.

The discrete form of this reference model is

$$\begin{aligned} \omega_{\text{ref}}(k+1) = &-\left(\frac{T_s\left(b_e + b_m\right)}{J_e' + J_m'} + \frac{T_s a_1}{\left(J_e' + J_m'\right)i^2} - 1\right)\omega_{\text{ref}}(k) \\ &+ \frac{T_s T_{\text{dem}}}{J_e' + J_m'} - \frac{T_s T_{wh0}}{\left(J_e' + J_m'\right)i}. \end{aligned} \tag{27}$$

Thus, the reference speed $\omega_{\text{ref}}(k)$ can be obtained from (27). $\omega_{\text{ref}}(k)$ is just the value of ω_{ref} at the sample time k in Figure 2, and $r(k) = \left[\omega_{\text{ref}}(k) \quad \omega_{\text{ref}}(k)\right]^T$ will be used as the reference (i.e., the set-point signal) of the motor speed $\omega_m(k)$ and the engine speed $\omega_e(k)$ in the model predictive controller.

The objective is then changed to find the best control vector ΔU to minimize the error function between the set-point and the predicted output. The cost function J that reflects the control objective is defined as

$$\begin{aligned} J &= \left(R_s - Y\right)^T\left(R_s - Y\right) + \Delta U^T\overline{R}\Delta U \\ &= \sum_{i=1}^{3}\left(\omega_{\text{ref}}(k) - \omega_m(k+i \mid k)\right)^2 + \left(\omega_{\text{ref}}(k) - \omega_e(k+i \mid k)\right)^2 \\ &\quad + r_{w1}\left(\Delta T_m(k)\right)^2 + r_{w2}\left(\Delta T_c(k)\right)^2 + r_{w3}\left(\Delta T_e(k)\right)^2. \end{aligned} \tag{28}$$

In the above equation, R_s is a data vector that contains the set-point information, and the weight matrix $\overline{R}$ is a diagonal matrix whose elements are used as the tuning parameters for the desired closed-loop performance:

$$\begin{aligned} R_s &= \left[\omega_{\text{ref}}(k) \quad \omega_{\text{ref}}(k) \quad \omega_{\text{ref}}(k) \quad \omega_{\text{ref}}(k) \quad \omega_{\text{ref}}(k) \quad \omega_{\text{ref}}(k)\right]^T, \\ \overline{R} &= \begin{bmatrix} r_{w1} & 0 & 0 \\ 0 & r_{w2} & 0 \\ 0 & 0 & r_{w3} \end{bmatrix}, \end{aligned} \tag{29}$$

where positive constants r_{w1}, r_{w2}, and r_{w3} are used to restrict the drastic changes of $T_m(k)$, $T_c(k)$, and $T_e(k)$, respectively.

The necessary condition of the minimum J is obtained as $\partial J/\partial\Delta U = 0$, from which the optimal control increment within one optimization window is shown as

$$\Delta U = \left(\phi^T\phi + \overline{R}\right)^{-1}\left(\phi^T\overline{R}_s r(k) - \phi^T F x(k)\right), \tag{30}$$

where $\phi^T\overline{R}_s$ is equal to the last two columns of $\phi^T F$.

From (30), it can be seen that the performance of the designed model predictive controller is affected by the choice of tuning parameters r_{w1}, r_{w2}, and r_{w3}. For example, the clutch torque change rate and the clutch frictional losses caused by (30) may be affected by r_{w2} to a large extent, which will be analyzed in the sensitivity analysis in Section 4.

4. Simulation Results

This section consists of three parts: (1) the simulation results to compare the proposed novel torque coordination control strategy with the conventional method; (2) sensitivity analysis of the selection of parameters on the mode transition performance in the proposed strategy; and (3) adaptiveness analysis of the proposed strategy.

Vehicle jerk, driveline torque interruption, and clutch frictional losses are crucial indices for mode transition performance. Vehicle jerk indicates smoothness, which is measured by the derivative of the vehicle acceleration. Vehicle

acceleration quantitatively describes the driveline torque interruption. Vehicle jerk and driveline torque interruption represent the longitudinal dynamics of a HEV. Clutch frictional losses can negatively affect the service life of clutch in a HEV. Let $|j|$ be the absolute value of vehicle jerk. The recommended value of $|j|$ is 10 m/s^3 in Germany and 17.64 m/s^3 in China [29]. Clutch frictional losses can be calculated by using the following formula [30]:

$$W_{sl} = \int_{t_0}^{t_f} T_c \left|\omega_e - \omega_m\right| dt, \tag{31}$$

where W_{sl} is the clutch friction work, $\omega_e - \omega_m$ stands for the speed difference of the two sides of clutch, and t_0 and t_f are the initial time and the terminal time of the slipping friction phase, respectively.

In order to verify the proposed novel torque coordination control strategy, the numerical simulations are carried out within MATLAB. The following simulations are conducted by using the nominal parameters of a hybrid electric car [14]: $m = 2300$ kg, $\alpha = 0$, $f_r = 0.02$ (ordinary concrete pavement), $R = 0.308$ m, $J_m = 0.22$ kg·m^2, $J_c = 0.05$ kg·m^2, $J_{gb} = 0.1$ kg·m^2, $J_e' = 0.4$ kg·m^2, $a_1 = 0.4$, $i = 5$, $b_m = 0.005$ N·m·s/rad, $b_e = 0.1$ N·m·s/rad, $T_s = 0.01$ s, $r_{w1} = 1$, $r_{w2} = 4$, $r_{w3} = 3$.

4.1. Comparison with the Conventional Method. HEV drivers have found that the transition time and power interruption can be reduced by pressing the accelerator pedal gradually and then releasing the clutch pedal quickly during the mode transition from pure electric running to parallel hybrid operation [18]. To evaluate the performance of the proposed novel torque coordination control strategy, this conventional method will be used as the baseline. The algorithm of the baseline operation is given by

$$T_m = T_{\text{dem}}, \qquad T_c = -300t, \qquad T_e = T_{e0} + 30t. \tag{32}$$

The equivalent driver's demand torque with respect to gearbox input side T_{dem} is shown in Figure 3. Besides, Figures 4~10 show the results of the proposed novel torque coordination control strategy and the baseline operation.

As shown in Figure 4, the mode transition duration of the novel strategy is 0.59 s longer than that of the baseline, but the slipping friction duration of clutch in the novel strategy is 0.09 s shorter than that of the baseline (the specific index is shown in Table 1), which is helpful to reduce the clutch frictional losses.

The absolute value of jerk amplitude in the novel strategy is far less than that of the baseline as shown in Figure 5 (the specific index is shown in Table 1). The reason for the smaller jerk of the novel strategy at 0.68 s is that the speed difference of the two sides of clutch has reached a small threshold value. For the novel strategy, the clutch synchronization point occurs at 0.91 s. Before this point, the set-point signal of the novel strategy comes from the reference model which happens to be the state-space equation behind the point, so very small jerk appears at the synchronization point.

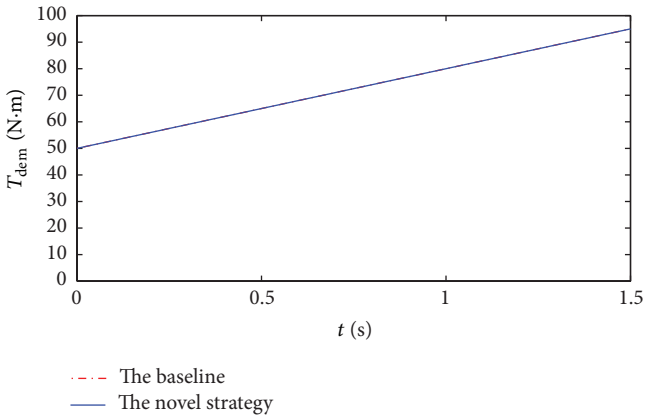

Figure 3: Equivalent driver's demand torque with respect to gearbox input side.

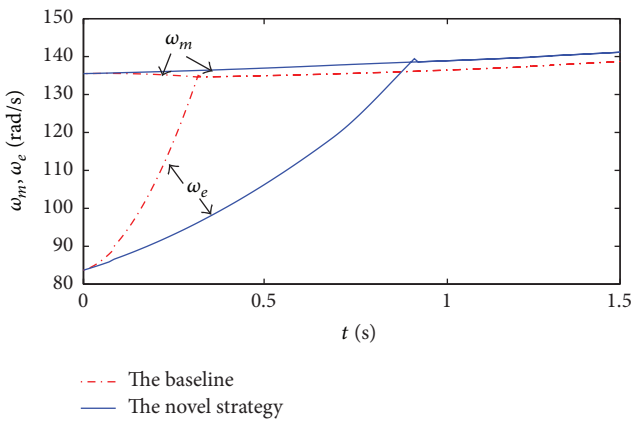

Figure 4: Angular speed of motor and engine.

As shown in Figure 6, vehicle acceleration of the novel strategy maintains a more stable fluctuation range than that of the baseline (the specific index is shown in Table 1).

Since vehicle jerk and driveline torque interruption are the indices of longitudinal dynamics of vehicles, both Figures 5 and 6 can prove that the proposed novel torque coordination control strategy is able to significantly improve HEV's smoothness and dynamic performance.

Figure 7 further indicates that the vehicle speed of the novel strategy changes more smoothly than that of the baseline, and this will improve HEV's driving comfort greatly.

Figure 8 shows that the clutch frictional losses resulting from the novel strategy are much less than those of the baseline operation (the specific index is shown in Table 1). All three factors in formula (31) are much less in the novel strategy than in the baseline; therefore, the clutch frictional losses are greatly reduced so that the proposed novel strategy is helpful to prolong the service life of clutch.

Figures 9 and 10 show that the proposed novel strategy increases the motor torque and the engine torque to compensate the negative clutch torque so that the smooth mode transition can be achieved.

Table 1: The specific indices of the proposed novel strategy and the baseline.

	The novel strategy	The baseline
The mode transition duration	0.91 s	0.32 s
The slipping friction duration of clutch	0.23 s (from 0.68 to 0.91 s)	0.32 s (from 0 to 0.32 s)
The absolute value of jerk amplitude	1.6 m/s^3	56 m/s^3
The fluctuation range of vehicle acceleration	0.14~0.26 m/s^2	−0.46~0.12 m/s^2
The clutch frictional losses	7.47 J	397.96 J

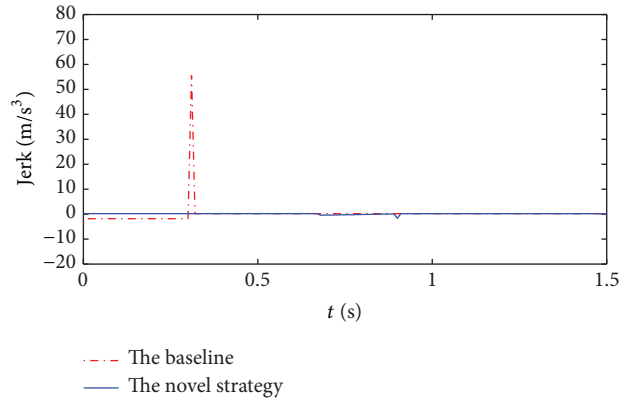

Figure 5: Vehicle jerk.

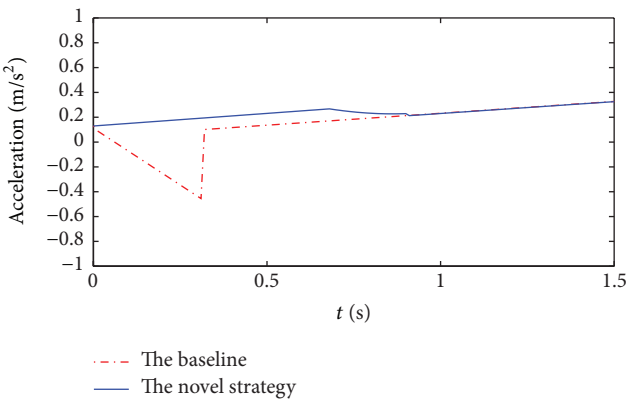

Figure 6: Vehicle acceleration.

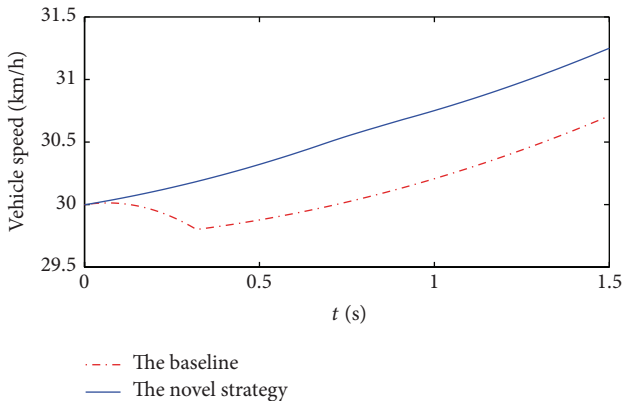

Figure 7: Vehicle speed.

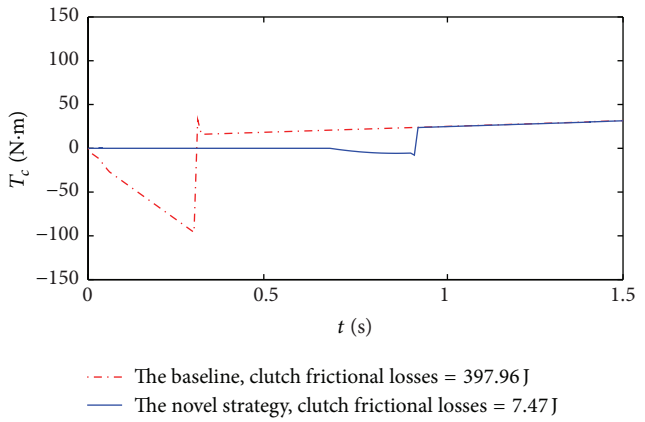

Figure 8: Clutch torque T_c.

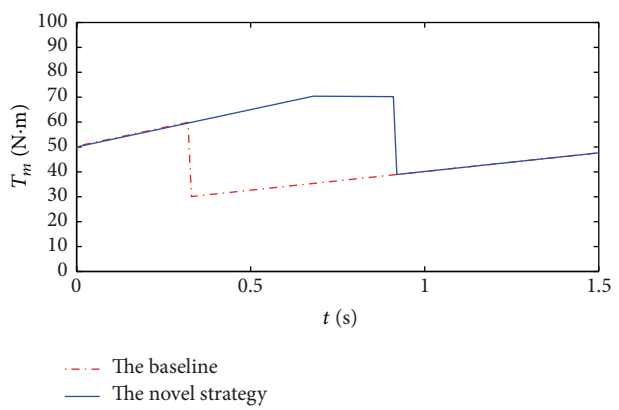

Figure 9: Motor torque T_m.

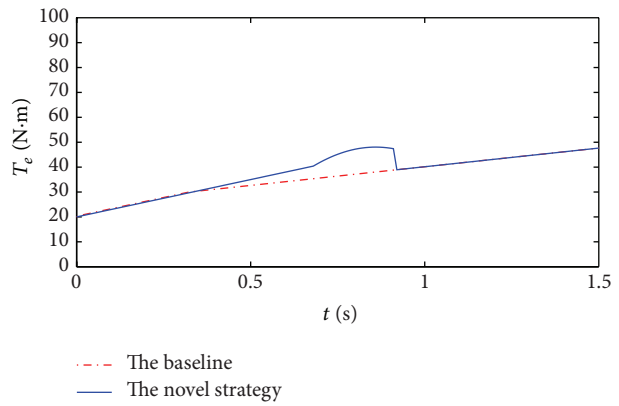

Figure 10: Engine torque T_e.

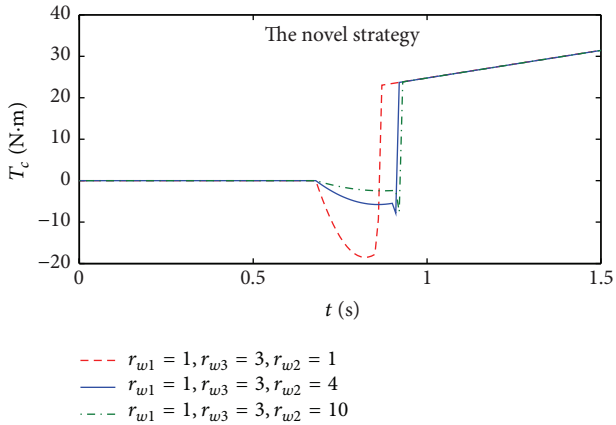

Figure 11: Clutch torque T_c under different tuning parameters r_{w2}.

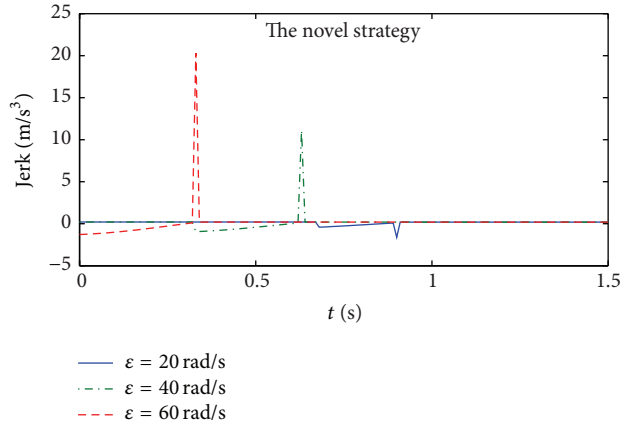

Figure 12: Vehicle jerk under different switch trigger ε.

4.2. Sensitivity Analysis of the Proposed Novel Torque Coordination Control Strategy. Several key parameters that may influence the mode transition performance are to be studied in this section for better performance of the proposed novel strategy.

4.2.1. Effect of the Tuning Parameter r_{w2} on Clutch Frictional Losses. Figure 11 shows the punishment role of different tuning parameters r_{w2} on clutch torque T_c. Here, r_{w2} is chosen to be 1, 4, and 10, respectively, and the other parameters remain the same. The resulting clutch frictional losses of the novel strategy which are calculated according to formula (31) are 20.56 J, 7.47 J, and 3.33 J, separately. Besides, the slipping friction duration is 0.18 s, 0.23 s, and 0.24 s, respectively. It can be seen that the bigger the tuning parameter r_{w2} is, the slower the clutch torque change is, the smaller the clutch torque is, and the smaller the clutch frictional losses are. But the slipping friction duration becomes longer as r_{w2} increases. Therefore, the proposed novel torque coordination strategy is sensitive to r_{w2}, so r_{w2} should be carefully chosen. Considering these factors comprehensively, $r_{w2} = 4$ is assumed.

4.2.2. Effect of the Switch Trigger ε on the Vehicle Jerk and Clutch Frictional Losses. The control role of different switch trigger ε on the vehicle jerk and clutch frictional losses is shown in Figures 12 and 13, respectively. It can be seen that the proposed novel strategy is sensitive to different ε. Figure 12 shows that the bigger the switch trigger is, the larger the vehicle jerk is.

As shown in Figure 13, small switch trigger implies less usage of clutch torque. The choice of small switch trigger is helpful for reducing slipping friction duration and frictional losses. However, the smaller the switch trigger is, the longer the mode transition time is. Taking sensor inaccuracy and actuator delay into account, it is impractical to choose ε too small.

4.3. Adaptiveness Analysis of the Proposed Novel Torque Coordination Control Strategy. For a running HEV, the mode transition from pure electric running to parallel hybrid operation may occur under different inclination angles, tire rolling resistance coefficients, vehicle masses, driving styles, and so on. As examples, the adaptiveness of the proposed novel strategy to different tire rolling resistance coefficients and driving styles is to be studied in this section.

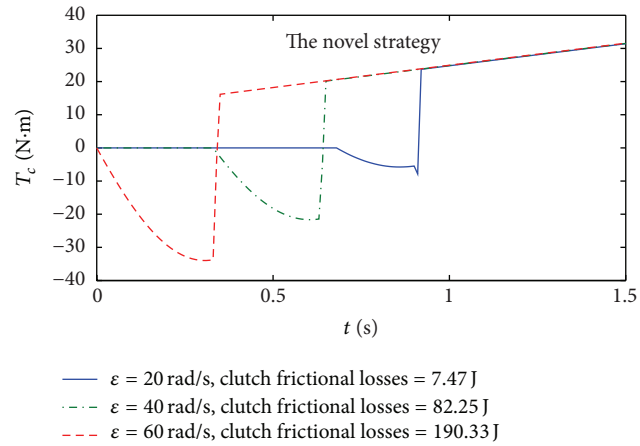

Figure 13: Clutch torque T_c and corresponding clutch frictional losses under different switch trigger ε.

4.3.1. The Adaptiveness of the Proposed Novel Strategy to Different Tire Rolling Resistance Coefficients. The tire rolling resistance coefficient f_r is equal to 0.02 for ordinary concrete pavement, whereas f_r becomes 0.04 for snow road. Figures 14 and 15 show that the absolute values of vehicle jerk and the clutch frictional losses are all very small in the case of either $f_r = 0.01$, $f_r = 0.02$, or $f_r = 0.04$. This indicates that the proposed novel strategy is adaptive to different tire rolling resistance coefficients.

4.3.2. The Adaptiveness of the Proposed Novel Strategy to Different Driving Styles. Vehicle jerk and clutch torque under different driving styles are shown in Figures 16 and 17, respectively. The change rates of acceleration pedal 30 N·m/s, 50 N·m/s, and 70 N·m/s mimic a mild driver, a normal driver, and an aggressive driver, respectively. Simulation results show

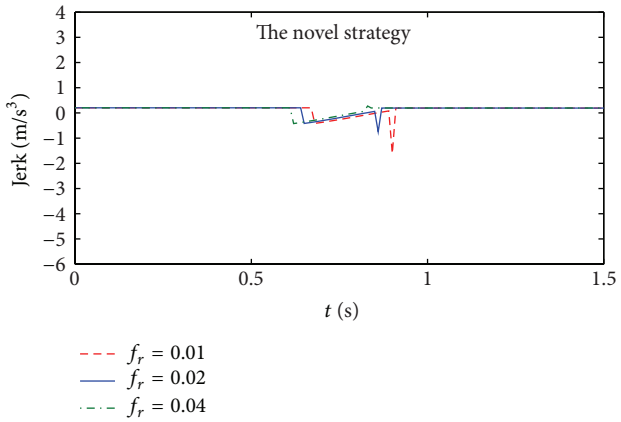

FIGURE 14: Vehicle jerk under different tire rolling resistance coefficient f_r.

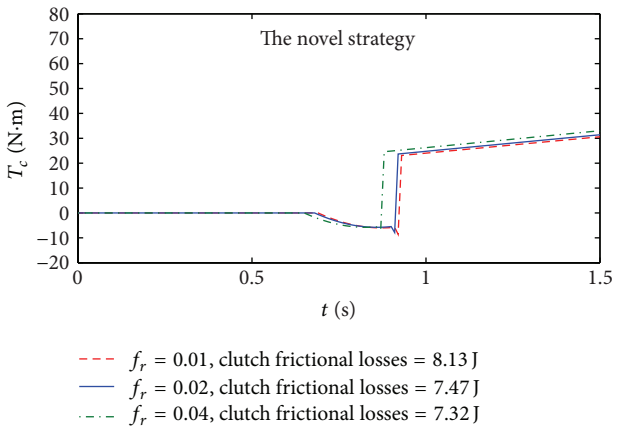

FIGURE 15: Clutch torque T_c and corresponding clutch frictional losses under different tire rolling resistance coefficient f_r.

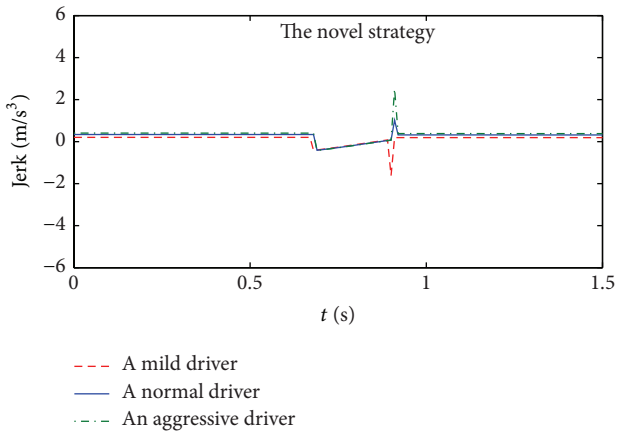

FIGURE 16: Vehicle jerk under different driving styles.

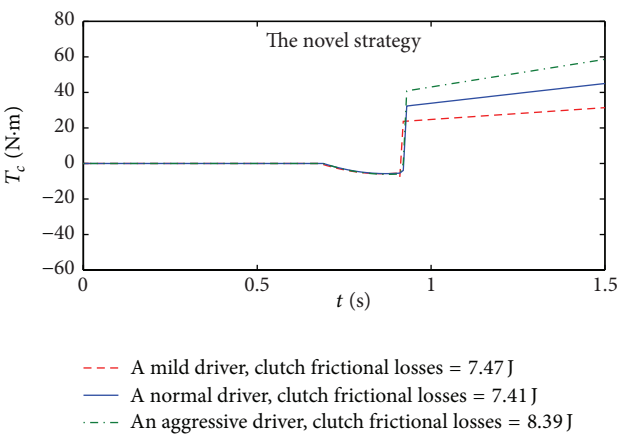

FIGURE 17: Clutch torque T_c and corresponding clutch frictional losses under different driving styles.

that the vehicle jerk and the clutch frictional losses are all very small which demonstrate that the proposed novel strategy is adaptive to different driving styles.

5. Conclusions

This paper proposes a novel torque coordination control strategy to achieve smooth mode transition from pure electric running to parallel hybrid operation for a single-shaft parallel HEV effectively. Compared with the existing MPC methods about torque coordination control, only one model predictive controller is needed, which reduces the calculation amount of the control strategy and is more suitable for the real-time control application. Since the clutch torque plays a crucial role for the improvement of transition performance, it is used as an optimized variable rather than a known parameter as in the existing MPC methods. Using the precious idea of MRC for reference, the desired performance during the mode transition is expressed by a reference model which directly generates the set-point signal of MPC real-timely. HEV's dynamic models under different running modes have been developed for the proposed novel strategy.

Compared with the baseline operation, the proposed novel torque coordination control strategy can achieve much smoother mode transition with much higher driving comfort, much better dynamic performance, and much lower clutch abrasion. The service life of clutch is greatly prolonged so that the use cost of HEV can be reduced. Several factors that may influence the performance of the proposed novel strategy have been studied through simulations. The proposed novel torque coordination control strategy is found to be sensitive to the tuning parameter r_{w2} and the threshold value of ε. ε is proved to have significant influence on vehicle jerk and clutch frictional losses. Further simulations have shown that the proposed novel strategy is adaptive to different tire rolling resistance coefficients and driving styles. The proposed novel torque coordination strategy will lay a foundation for the practical application in HEV control units. There are some physical constraints in HEV. For example, the engine torque T_e, the clutch friction torque T_c, the motor torque T_m, and their change rates are all bounded. So far, these constraints are not concerned in this paper. Future work will address the model predictive controller with HEV's realistic constraints.

Conflict of Interests

The authors declare that there is no conflict of interests regarding the publication of this paper.

Acknowledgments

This work was supported by the National Natural Science Foundation of China (Grant nos. 61034007, 51277116, 61403236, 61304130, and 61304029), the Natural Science Foundation of Xinjiang (Grant no. 201318101-16).

References

[1] S. Kermani, R. Trigui, S. Delprat, B. Jeanneret, and T. M. Guerra, "PHIL implementation of energy management optimization for a parallel HEV on a predefined route," *IEEE Transactions on Vehicular Technology*, vol. 60, no. 3, pp. 782–792, 2011.

[2] F. R. Salmasi, "Control strategies for hybrid electric vehicles: evolution, classification, comparison, and future trends," *IEEE Transactions on Vehicular Technology*, vol. 56, no. 5, pp. 2393–2404, 2007.

[3] Y. Zou, S.-J. Hou, D.-G. Li, W. Gao, and X.-S. Hu, "Optimal energy control strategy design for a hybrid electric vehicle," *Discrete Dynamics in Nature and Society*, vol. 2013, Article ID 132064, 8 pages, 2013.

[4] J. T. B. A. Kessels, M. W. T. Koot, P. P. J. van den Bosch, and D. B. Kok, "Online energy management for hybrid electric vehicles," *IEEE Transactions on Vehicular Technology*, vol. 57, no. 6, pp. 3428–3440, 2008.

[5] Y. Gurkaynak, A. Khaligh, and A. Emadi, "State of the art power management algorithms for hybrid electric vehicles," in *Proceedings of the 5th IEEE Vehicle Power and Propulsion Conference (VPPC '09)*, pp. 388–394, Dearborn, Mich, USA, September 2009.

[6] L.-H. Wu, Y.-N. Wang, X.-F. Yuan, and Z.-L. Chen, "Multi-objective optimization of HEV fuel economy and emissions using the self-adaptive differential evolution algorithm," *IEEE Transactions on Vehicular Technology*, vol. 60, no. 6, pp. 2458–2470, 2011.

[7] S. Ebbesen, P. Elbert, and L. Guzzella, "Battery state-of-health perceptive energy management for hybrid electric vehicles," *IEEE Transactions on Vehicular Technology*, vol. 61, no. 7, pp. 2893–2900, 2012.

[8] S. J. Moura, J. L. Stein, and H. K. Fathy, "Battery-health conscious power management in plug-in hybrid electric vehicles via electrochemical modeling and stochastic control," *IEEE Transactions on Control Systems Technology*, vol. 21, no. 3, pp. 679–694, 2013.

[9] Y. Tong, *Study on the coordinated control issue in parallel hybrid electric system [Ph.D. thesis]*, Tsinghua University, Beijing, China, 2004.

[10] R. I. Davis and R. D. Lorenz, "Engine torque ripple cancellation with an integrated starter alternator in a hybrid electric vehicle: implementation and control," *IEEE Transactions on Industry Applications*, vol. 39, no. 6, pp. 1765–1774, 2003.

[11] Q.-N. Wang, E.-C. Ji, and W.-H. Wang, "Coordinated control for mode-switch of parallel hybrid electric vehicle," *Journal of Jilin University: Engineering and Technology Edition*, vol. 38, no. 1, pp. 1–6, 2008.

[12] M.-H. Li, Y.-G. Luo, D.-G. Yang, K.-Q. Li, and X.-M. Lian, "A dynamic coordinated control method for parallel hybrid electric vehicle based on model matching control," *Automotive Engineering*, vol. 29, no. 3, pp. 203–207, 2007.

[13] L. Wang, Y. Zhang, J. Shu, and C. Yin, "Mode transition control for series-parallel hybrid electric bus using fuzzy adaptive sliding mode approach," *Journal of Mechanical Engineering*, vol. 48, no. 14, pp. 119–127, 2012.

[14] K. Koprubasi, E. R. Westervelt, and G. Rizzoni, "Toward the systematic design of controllers for smooth hybrid electric vehicle mode changes," in *Proceedings of the American Control Conference (ACC 07)*, pp. 2985–2990, July 2007.

[15] V. T. Minh and A. A. Rashid, "Modeling and model predictive control for hybrid electric vehicles," *International Journal of Automotive Technology*, vol. 13, no. 3, pp. 477–485, 2012.

[16] R. Beck, F. Richert, A. Bollig et al., "Model predictive control of a parallel hybrid vehicle drivetrain," in *Proceedings of the 44th IEEE Conference on Decision and Control, and the European Control Conference (CDC-ECC '05)*, pp. 2670–2675, December 2005.

[17] M. Song, J. Oh, and H. Kim, "Engine clutch control algorithm during mode change for parallel hybrid electric vehicle," in *Proceedings of the IEEE Vehicle Power and Propulsion Conference (VPPC '12)*, pp. 1118–1121, October 2012.

[18] L. Chen, G. Xi, and J. Sun, "Torque coordination control during mode transition for a series-parallel hybrid electric vehicle," *IEEE Transactions on Vehicular Technology*, vol. 61, no. 7, pp. 2936–2949, 2012.

[19] J. M. Maciejowski, *Predictive Control with Constraints*, Prentice-Hall, London, UK, 2001.

[20] X. B. Kong and X. J. Liu, "Nonlinear model predictive control for DFIG-based wind power generation," *Acta Automatica Sinica*, vol. 39, no. 5, pp. 636–643, 2013.

[21] S. Bolognani, S. Bologani, L. Peretti, and M. Zigliotto, "Design and implementation of model predictive control for electrical motor drives," *IEEE Transactions on Industrial Electronics*, vol. 56, no. 6, pp. 1925–1936, 2009.

[22] X. J. Liu, P. Guan, and C. W. Chan, "Nonlinear multivariable power plant coordinate control by constrained predictive scheme," *IEEE Transactions on Control Systems Technology*, vol. 18, no. 5, pp. 1116–1125, 2010.

[23] P. Falcone, F. Borrelli, J. Asgari, H. E. Tseng, and D. Hrovat, "Predictive active steering control for autonomous vehicle systems," *IEEE Transactions on Control Systems Technology*, vol. 15, no. 3, pp. 566–580, 2007.

[24] D. Hrovat, S. di Cairano, H. E. Tseng, and I. V. Kolmanovsky, "The development of model predictive control in automotive industry: a survey," in *Proceedings of the IEEE International Conference on Control Applications (CCA '12)*, pp. 295–302, October 2012.

[25] A. Myklebust and L. Eriksson, "Torque model with fast and slow temperature dynamics of a slipping dry clutch," in *Proceedings of the IEEE Vehicle Power and Propulsion Conference (VPPC '12)*, pp. 851–856, October 2012.

[26] L.-P. Wang, *Model Predictive Control System Design and Implementation Using MATLAB*, Springer, London, UK, 2009.

[27] E. F. Camacho and C. Bordons, *Model Predictive Control*, Springer, London, UK, 2007.

[28] Y.-G. Xi, *Predictive Control*, National Defence Industry Press, Beijing, China, 1993.

[29] L. Guo, A. Ge, T. Zhang, and Y. Yue, "AMT shift process control," *Transactions of the Chinese Society of Agricultural Machinery*, vol. 34, no. 2, pp. 1–3, 2003.

[30] J. W. Zhang, L. Chen, and G. Xi, "System dynamic modelling and adaptive optimal control for automatic clutch engagement of vehicles," *Proceedings of the Institution of Mechanical Engineers D: Journal of Automobile Engineering*, vol. 216, no. 12, pp. 983–991, 2002.